

## Supplemental Information

**Title: “Paclitaxel neurotoxicity is triggered by epidermal EG5 dependent microtubule fasciculation and X-ROS formation”**

### Authors:

Chia-Jung Hsieh<sup>1</sup>, Anthony M Cirrincione<sup>1</sup>, Mikaela R Vlach<sup>1</sup>, Antonio Cadiz Diaz<sup>1</sup>, Natalie A Schmidt<sup>1</sup>, Xin Li<sup>1</sup>, Sergio Gutierrez<sup>1</sup>, Marie J Ugo<sup>1</sup>, Maria Celina Amaya Sanchez<sup>2</sup>, Cassandra A. Reimonn<sup>3</sup>, Stefan Wuchty<sup>1,4</sup>, Adriana D Pellegrini<sup>5</sup>, Leah RK Rude<sup>5</sup>, Leah G Pappalardo<sup>5</sup>, Daniel P Regan<sup>6</sup>, Bowen Zhao<sup>7</sup>, Fuwu Zhang<sup>7</sup>, Caitlin Howell<sup>6</sup>, Sybil Hrstka<sup>8</sup>, Surendra Dasari<sup>8</sup>, Enrico Capobianco<sup>9</sup>, Thomas S Lisse<sup>1,10</sup>, Benjamin J Harrison<sup>3</sup>, Nathan P Staff<sup>8</sup>, Mike Xiangxi Xu<sup>2,10</sup> and Sandra Rieger<sup>1,10\*</sup>

### Affiliations:

<sup>1</sup>Department of Biology, University of Miami, Coral Gables, Florida 33146, USA

<sup>2</sup>Department of Cell Biology, University of Miami Miller School of Medicine, Miami, Florida 33136, USA

<sup>3</sup>University of New England, Department of Biomedical Sciences, Biddeford, Maine, 04005

<sup>4</sup>Department of Computer Science, University of Miami, Coral Gables, Florida 33146, USA

<sup>5</sup>MDI Biological Laboratory, Kathryn W. Davis Center for Regenerative Biology and Medicine, Bar Harbor, Maine 04762, USA

<sup>6</sup>Department of Chemical and Biomedical Engineering, University of Maine, Orono, Maine 04469, USA

<sup>7</sup>Department of Chemistry, Macdonald Foundation Biomedical Nanotechnology Institute, University of Miami, Coral Gables, Florida 33146, USA

<sup>8</sup>Department of Neurology, Mayo Clinic, Rochester, MN 55905, USA

<sup>9</sup>The Jackson Laboratory for Genomic Medicine, Farmington, CT 06032, USA

<sup>10</sup>Sylvester Comprehensive Cancer Center, University of Miami Miller School of Medicine, Miami, Florida 33136, USA

**\*Correspondence:** Email: [sriegeer@miami.edu](mailto:sriegeer@miami.edu)

### This PDF file includes:

Supplementary Text

Figs. S1 to S13

Movie legends S1 to S10

### Other Supplementary Materials for this manuscript include the following:

Movies S1 to S10

## Supplemental Figures & Legends

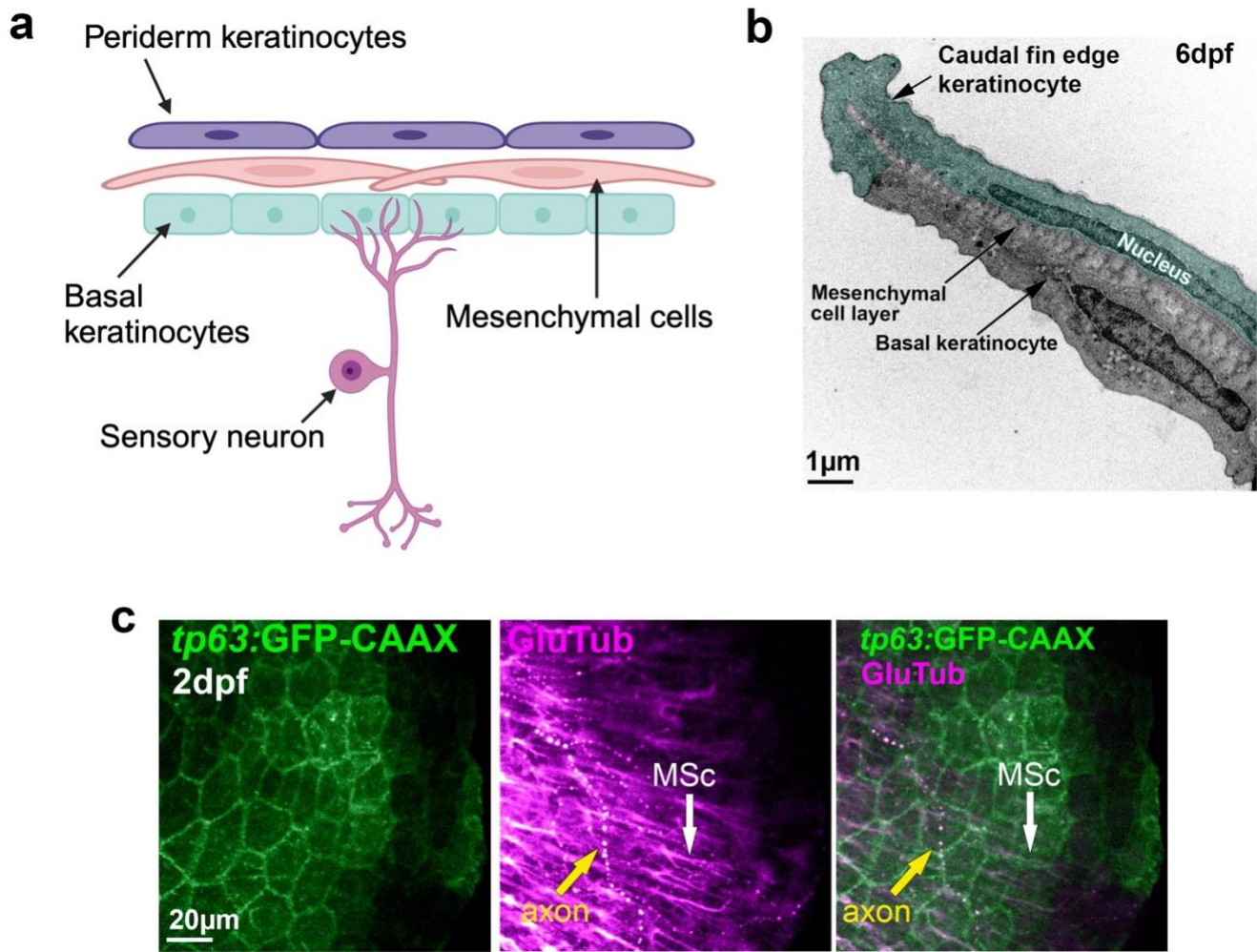


### Figure S1. Larval zebrafish caudal fin morphology.

(a) Schematic of the caudal fin. Mesenchymal cells (MSc) span across multiple keratinocytes, while cutaneous axons innervate the basal keratinocyte layer and branch between the basal and mesenchymal layers.

(b) Transmission electron microscopy of a 6dpf larval caudal fin reveals two epidermal layers: the outer periderm and inner basal keratinocytes, with medially located mesenchymal cells (MSc).

(c) Caudal fin of a 2dpf Tg(*tp63:GFP-CAAX*) fish showing GFP-labeled keratinocyte membranes stained for GluTub to detect deetyrosinated microtubules. Cutaneous sensory axons exhibit deetyrosination (yellow arrow, dotted structures), while MSc display elongated, bifurcating deetyrosinated microtubules (white arrow) spanning multiple keratinocytes.

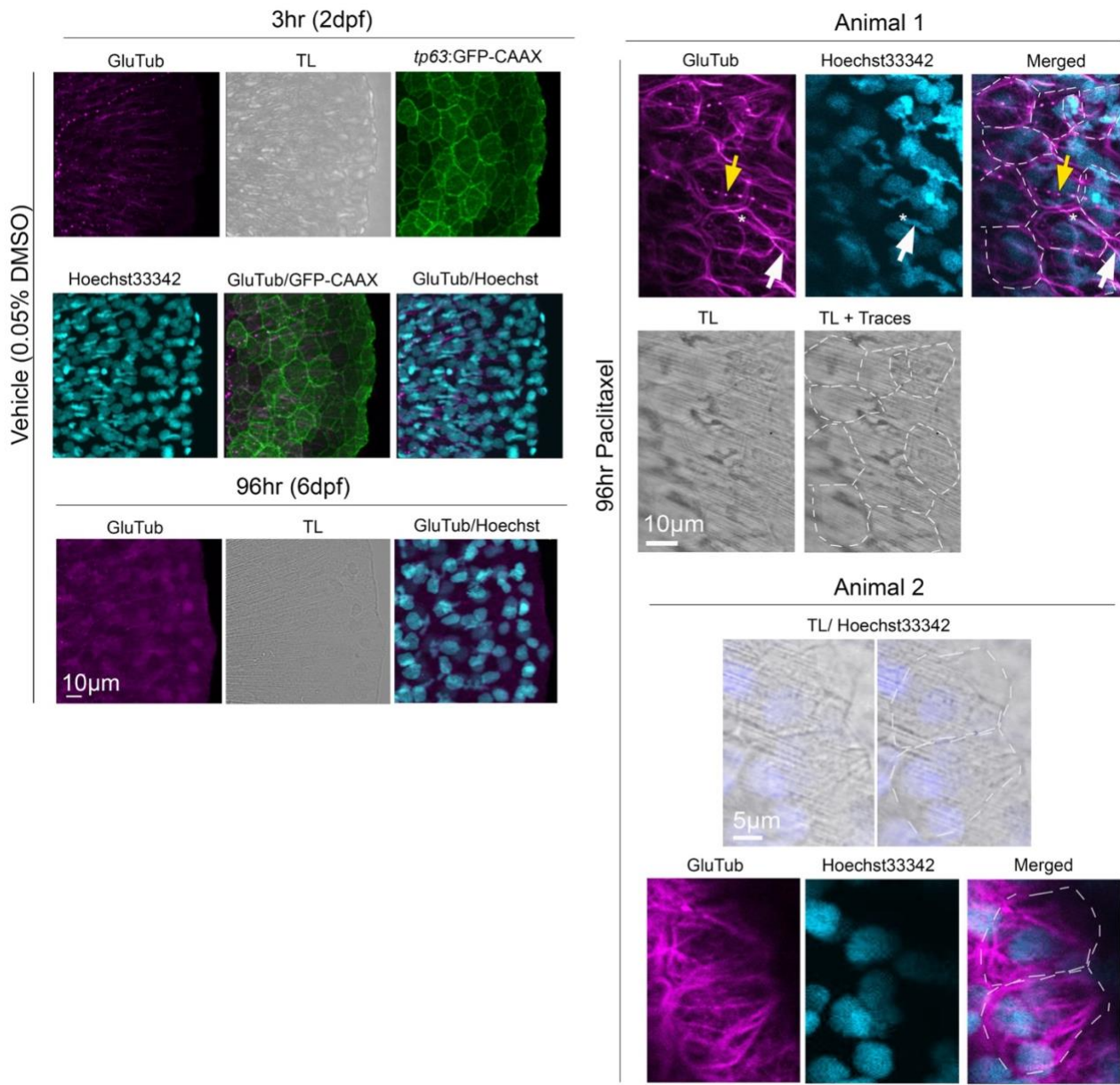


**Figure S2. Contextual view of keratinocyte membranes and fasciculated microtubules in the larval zebrafish caudal fin.**

**Left:** Vehicle-treated controls after 3hr (2dpf) and 96hr (6dpf) treatments. At 2dpf, GFP-CAAX (membrane-bound GFP) expression is visible in basal keratinocytes (driven by the *tp63* promoter). By 6dpf, GFP-CAAX is no longer detectable in the distal fin, so only GluTub and Hoechst 33342 staining are shown.

**Right:** Two animals stained for GluTub and Hoechst 33342 with corresponding transmitted light images shown at low (top) and high (bottom) magnification. Transmitted light images were used to draw keratinocyte outlines (dotted lines), overlaid onto fluorescent images showing fasciculated dMTs in magenta. **Animal 1:** Transmitted light panels are single slices; fluorescent panels are projected images to better illustrate structures. Yellow arrows indicate punctate dMT staining in an axon. White arrows mark fasciculated dMTs in a mesenchymal cell beneath the epidermis. Asterisks denote the elongated, irregular nuclei of mesenchymal cells, which contrast with the rounder keratinocyte nuclei. Mesenchymal dMTs are bifurcated and wrap around the nucleus, which appears narrower overall. **Animal 2:** Transmitted light panel with Hoechst33342 overlaid and in which cell borders are outlined. The same cells are shown as fluorescent images below in which dMTs are labeled and the outlines of the cells are demarcated.



## Maximum Intensity Projections

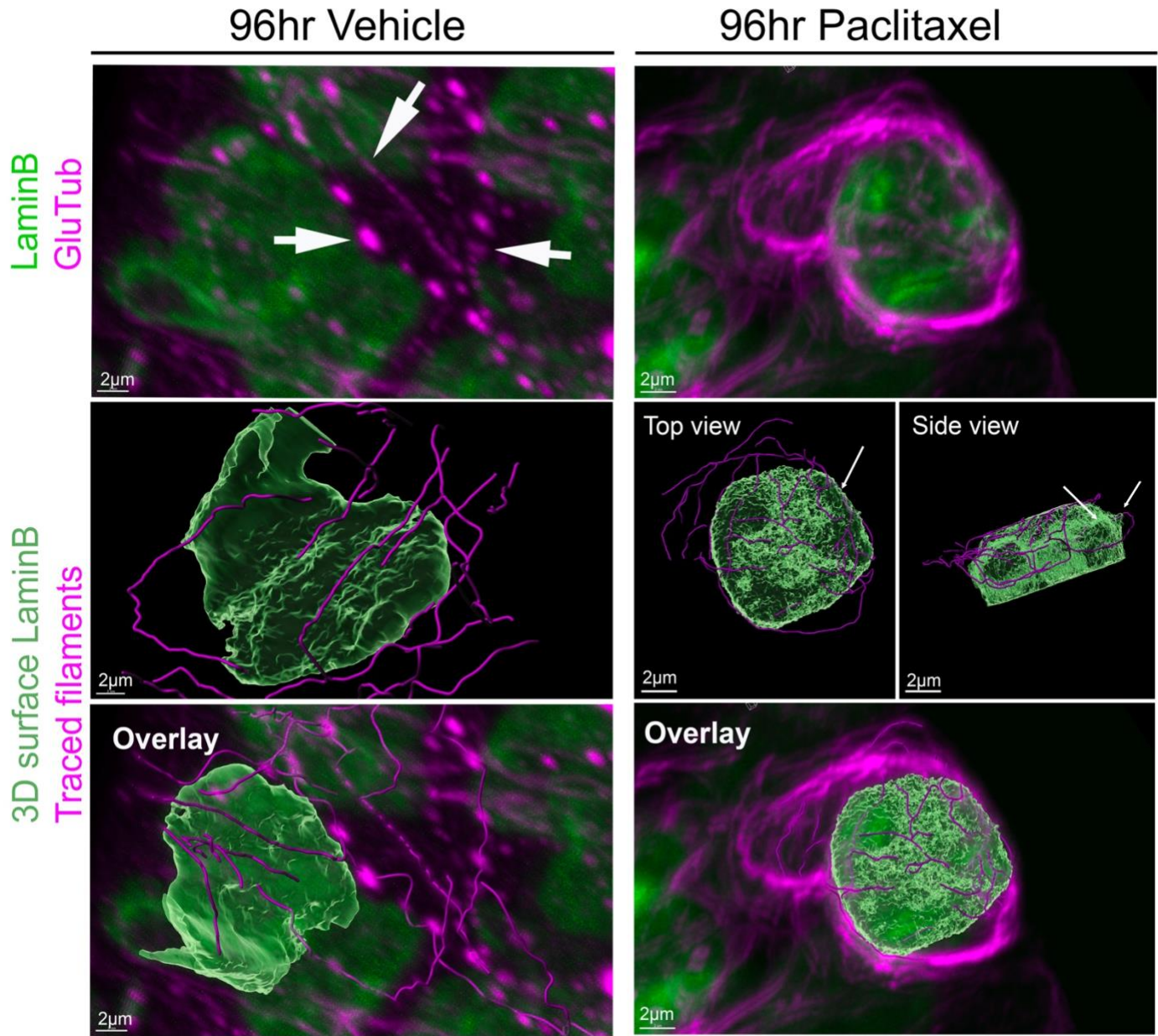


**Figure S3. Fasciculated detyrosinated microtubules traverse the nuclear lamina in zebrafish treated with paclitaxel for 96 hours.**

Whole-mount immunofluorescence with antibodies against Lamin B (nuclear lamina) and detyrosinated tubulin (GluTub) in zebrafish treated for 96hr either with vehicle (left) or paclitaxel (right). Maximum intensity projections of the distal caudal fin edge region are shown. The top panels show antibody staining whereas the panels below show 3D renderings of the panels above. The bottom panels show an overlay of both upper panels. *Left panels (Vehicle)*: Arrows in the vehicle-treated animal emphasize that the staining marks primarily cutaneous sensory axons that are GluTub positive (punctate staining) and which innervate the epidermis but do not traverse the nucleus given their distinct localization outside the cell. *Right panels (Paclitaxel)*: Thin arrows in the 3D rendered nucleus of the paclitaxel-treated animal point to dMTs piercing and entering the nucleus. See also **Movie S7**.

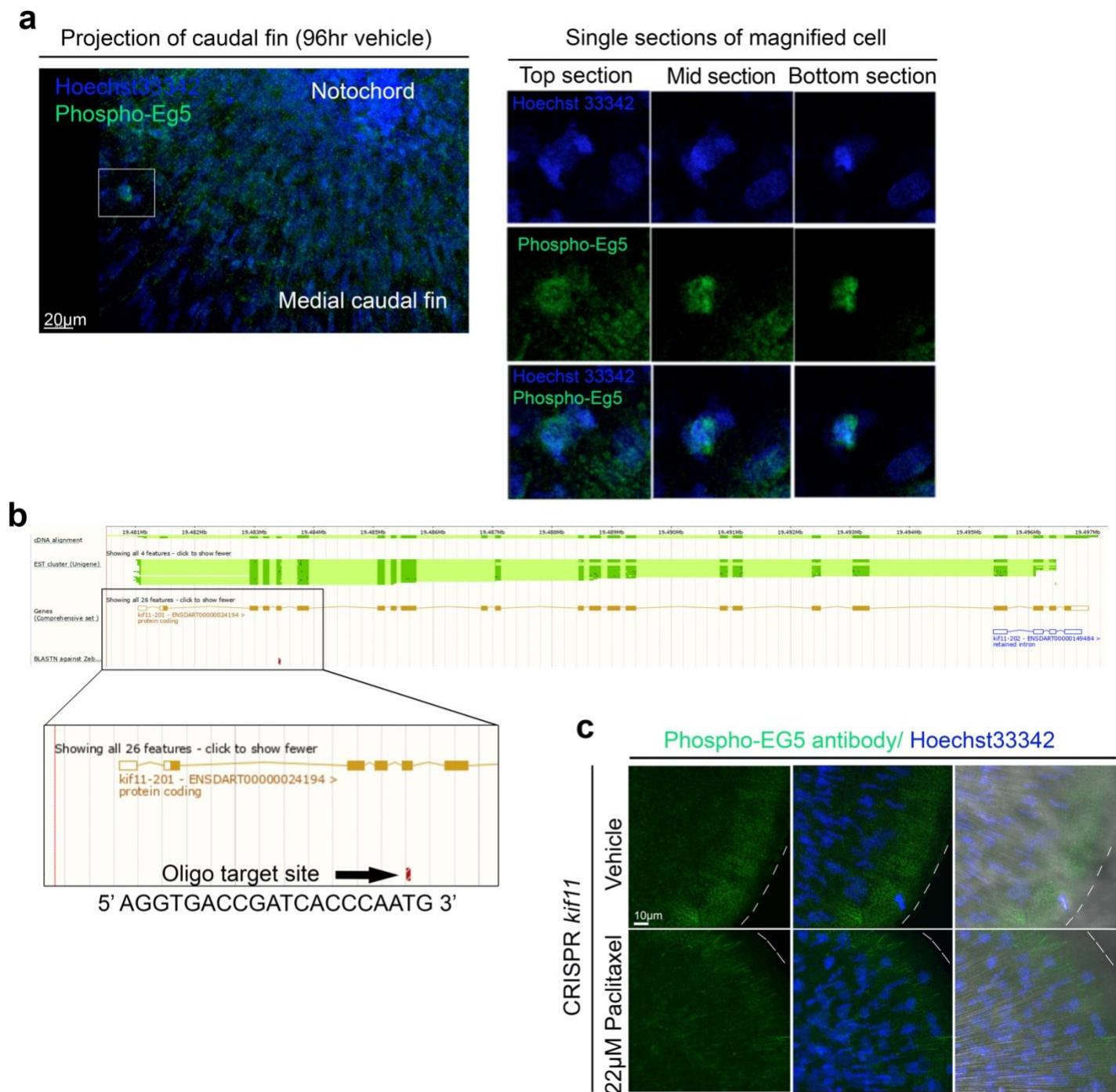


**Figure S4. Phospho-EG5 expression controls in vehicle and *kif11* CRISPR knockout fish.**

(a) Phospho-Eg5 staining in a dividing cell of a 96hr vehicle control animal. The top image shows a projected overview of a caudal fin midsection with a single cell showing condensed phospho-EG5 and nuclear material visualized with Hoechst33342. The bottom panels show the same cell at higher magnification in single slices (top, mid, bottom). The bright, compact Hoechst signal is seen in two distinct clusters of condensed DNA forming, consistent with condensed chromosomes. Phospho-EG5 signal is co-localized with condensed chromatin.

(b) Zebrafish *kif11* gene and oligo target site.

(c) 96hr vehicle (top) and paclitaxel (bottom) treatment reveals the absence of Eg5 expression in caudal fin keratinocytes following *kif11* CRISPR oligo injection into 1-cell stage embryos.



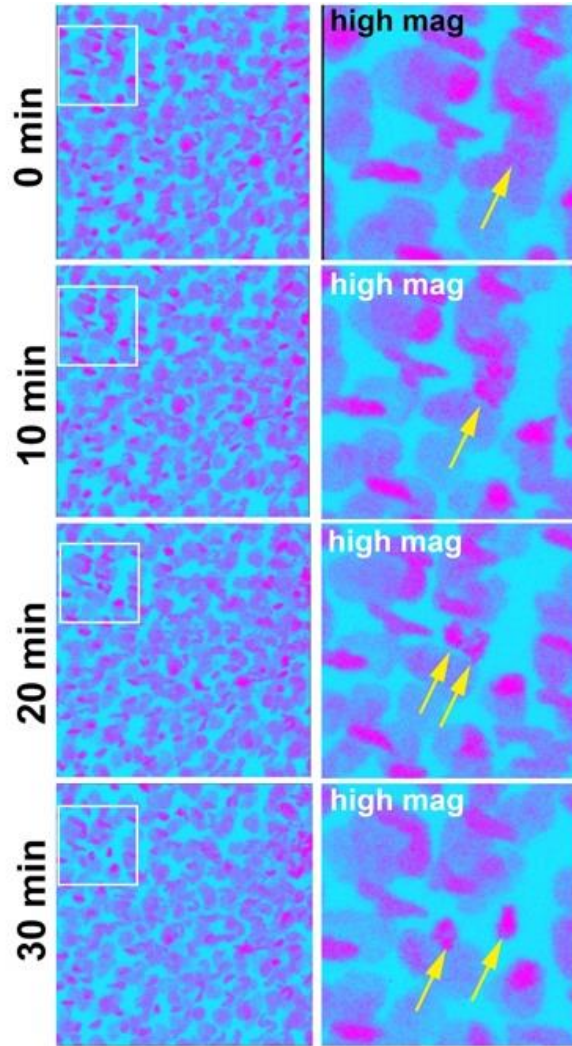


**Figure S5. Keratinocyte division in larval caudal fin.** Time-lapse recording of dividing keratinocyte (yellow arrows) over the course of 30 minutes in the caudal fin of a 6dpf *Tg(h2a-h2a:GFP)* transgenic larval zebrafish.

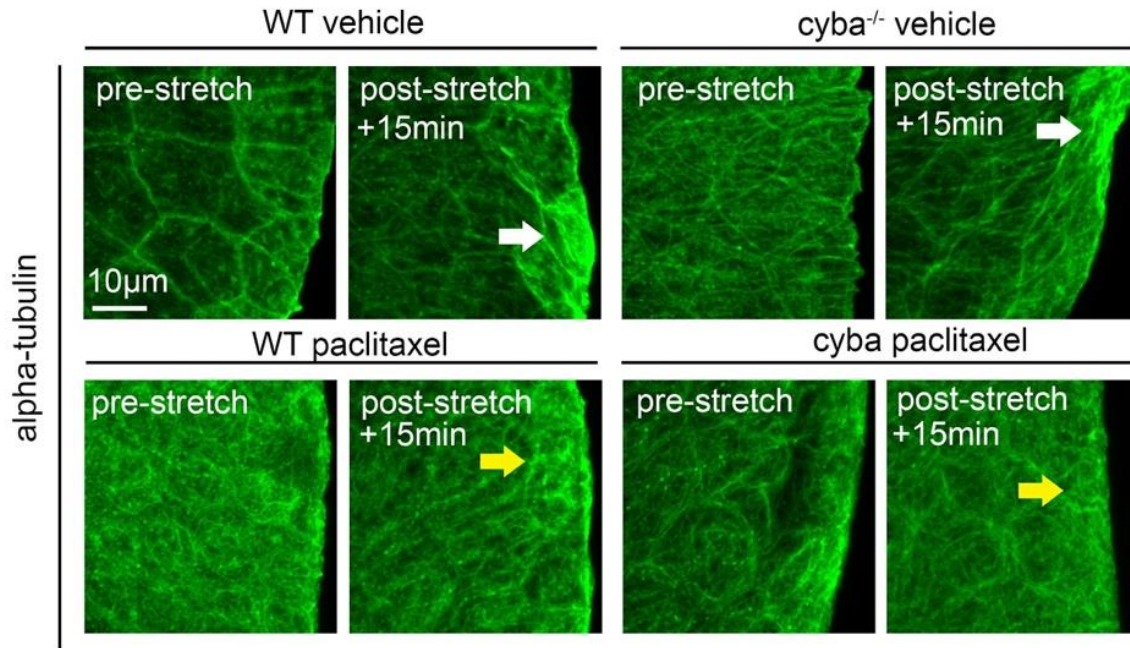


**Figure S6. Validation of ZStretcher in larval zebrafish.**

(Top) Immunofluorescence staining for alpha-tubulin reveals stretched microtubules at the fin edge (white arrows) in both wildtype and homozygous *cyba*<sup>-/-</sup> zebrafish after 48-hour vehicle treatment.

(Bottom) This microtubule stretching is reduced in both genotypes following paclitaxel treatment (yellow arrows).

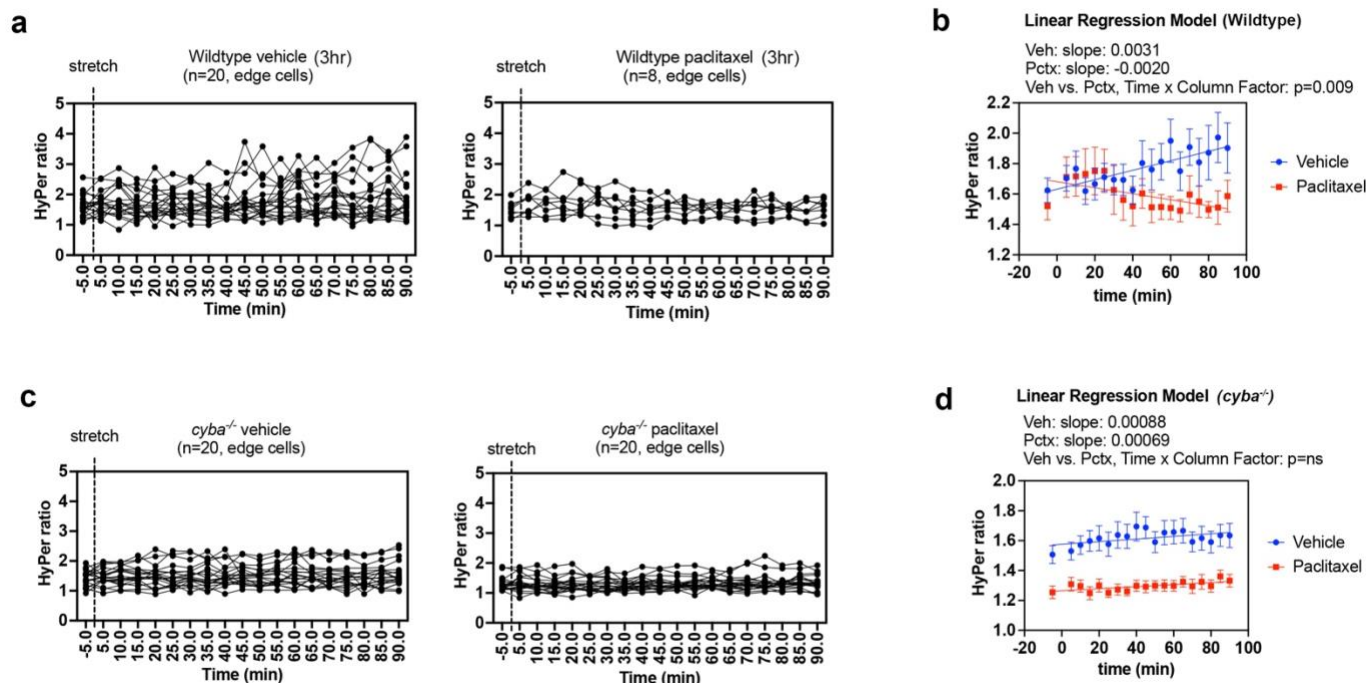


**Figure S7. Stretch data analysis.**

(a) Wildtype vehicle (left) and paclitaxel (right) treatments shown as individual curves.

(b) Linear regression analysis for each wildtype treatment group. Time x Column statistics is shown for vehicle versus paclitaxel treatment, showing significance.

(c) *cyba*<sup>-/-</sup> vehicle (left) and paclitaxel (right) treatments shown as individual curves.

(d) Linear regression analysis for each *cyba*<sup>-/-</sup> treatment group. Linear regression statistics are shown for vehicle versus paclitaxel treatment, showing no significance.



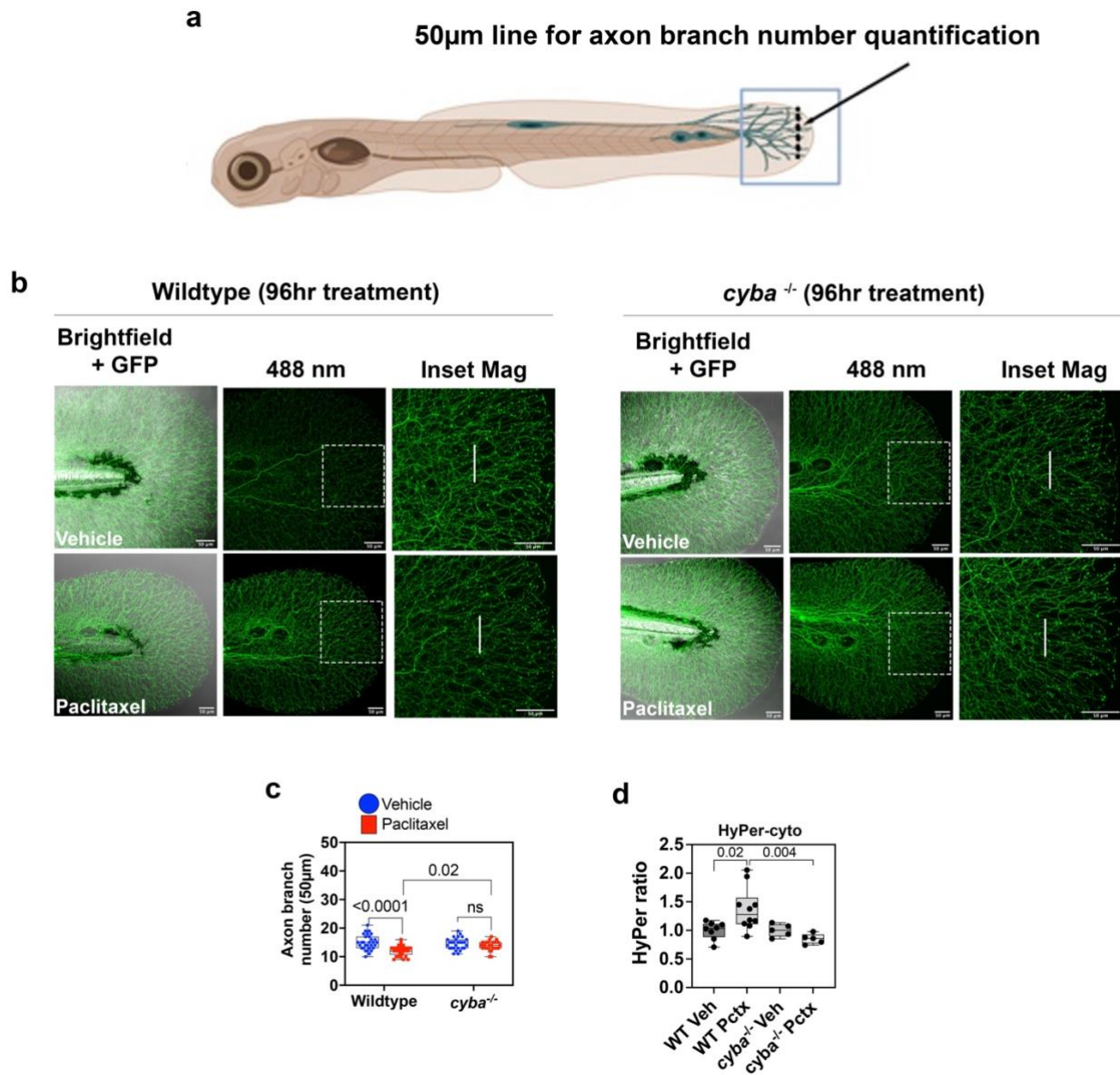


**Figure S8. Rescue of neurotoxicity and H<sub>2</sub>O<sub>2</sub> formation in paclitaxel-treated *cyba*<sup>-/-</sup> mutants.**

(a) *Tg(isl2b:GFP)* wildtype and homozygous *cyba*<sup>-/-</sup> zebrafish were treated from 2–6dpf with either vehicle (0.05% DMSO) or paclitaxel. RB sensory neuron axons innervating the caudal fin are shown. A 50µm line marks the region where cutaneous axon branches were quantified, located 100µm from the distal fin edge.

(b) Quantification of axon branches shows reduced branching in paclitaxel-treated wildtype fish, an effect prevented in *cyba*<sup>-/-</sup> mutants.

(c) HyPer imaging reveals increased H<sub>2</sub>O<sub>2</sub> oxidation in keratinocytes of paclitaxel-treated wildtype fish, but not in *cyba*<sup>-/-</sup> mutants.

(d) HyPer-cyto ratio in wildtype and *cyba* mutants confirms the absence of H<sub>2</sub>O<sub>2</sub> formation in the mutants following 96hr of treatment either with vehicle or paclitaxel.

Abbreviations: Mag, magnification; WT, wildtype; Pctx, paclitaxel; Veh, vehicle (0.05% DMSO).

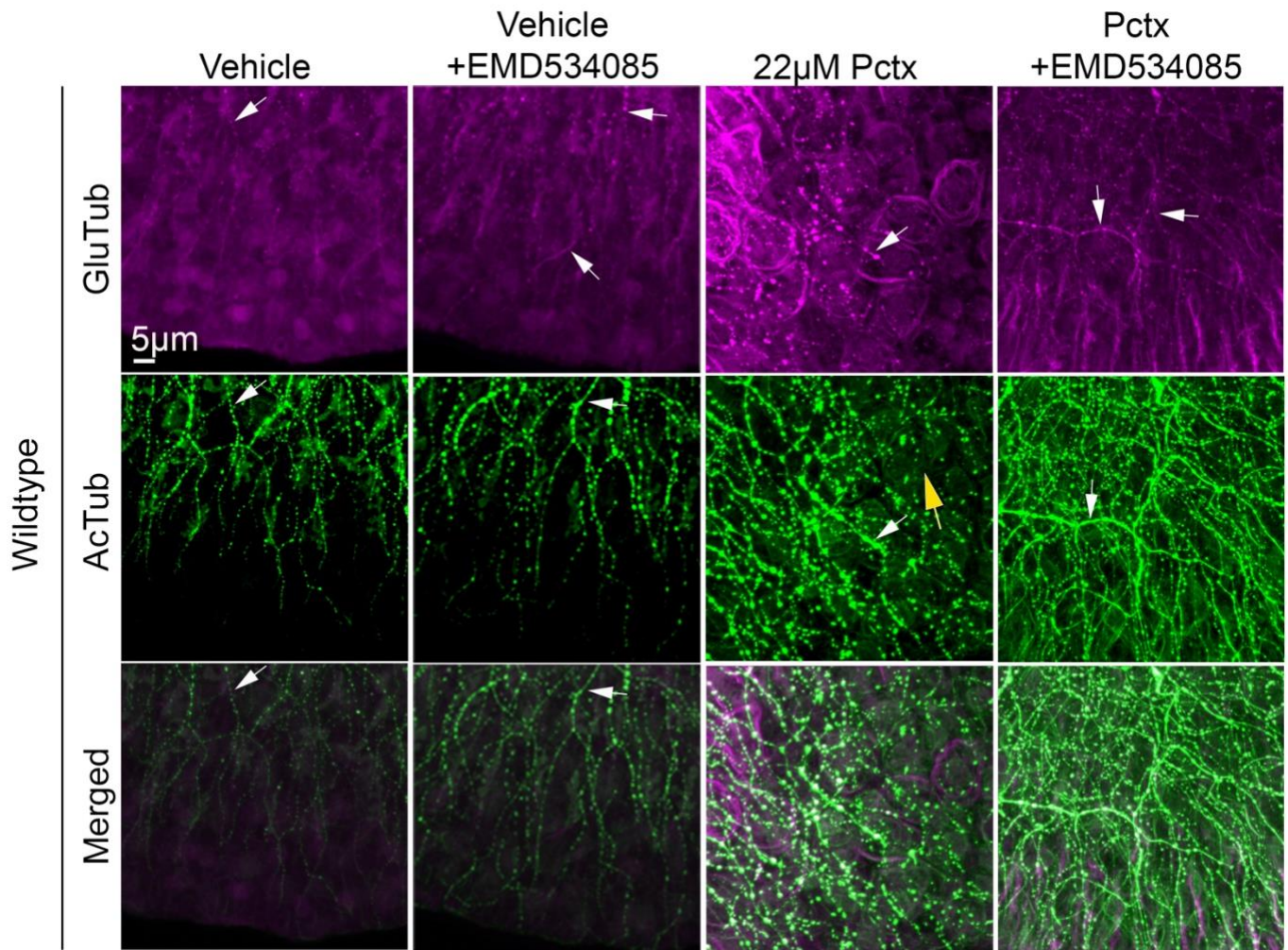


**Figure S9. Paclitaxel enhances axonal detyrosination and keratinocyte acetylation independent of EG5.**

Weak axonal detyrosination (GluTub, white arrows) is observed in vehicle-treated animals and those receiving vehicle+EMD534085. Paclitaxel increases axonal detyrosination regardless of EMD534085 co-treatment (white arrows). Keratinocyte-specific acetylation (AcTub) is increased in both axons (white arrows) and keratinocytes (yellow arrows) after 96hr of paclitaxel treatment. Co-treatment with paclitaxel+EMD534085 slightly reduces keratinocyte, but not axonal, acetylation compared to paclitaxel alone.

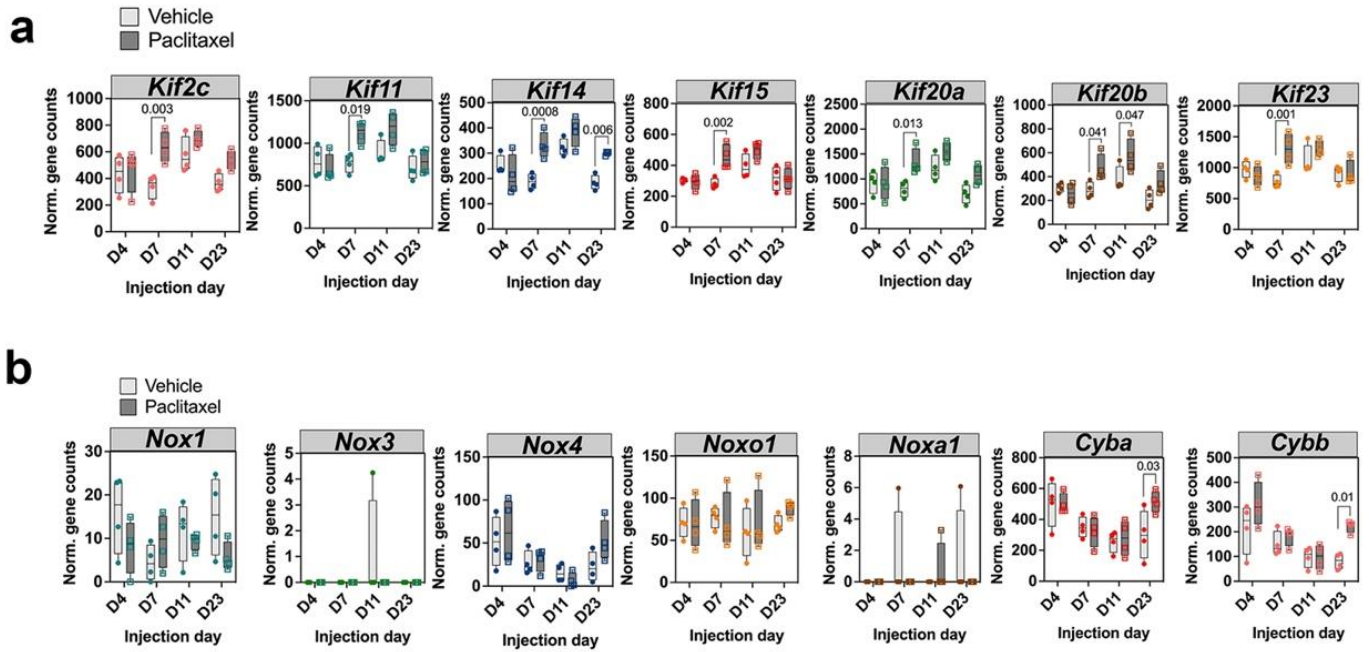


**Figure S10. Kif and Nox gene expression in mouse RNAseq dataset.**

RNAseq was performed on glabrous skin from mouse hind paws.

(a) Normalized gene counts show that multiple *Kif* genes are upregulated following paclitaxel treatment, with peak expression at Days 7 and 11.

(b) Normalized counts for Nox genes and regulatory subunits *Cyba* and *Cybb*. Only *Cyba* and *Cybb* are significantly upregulated, and this occurs during the recovery phase.



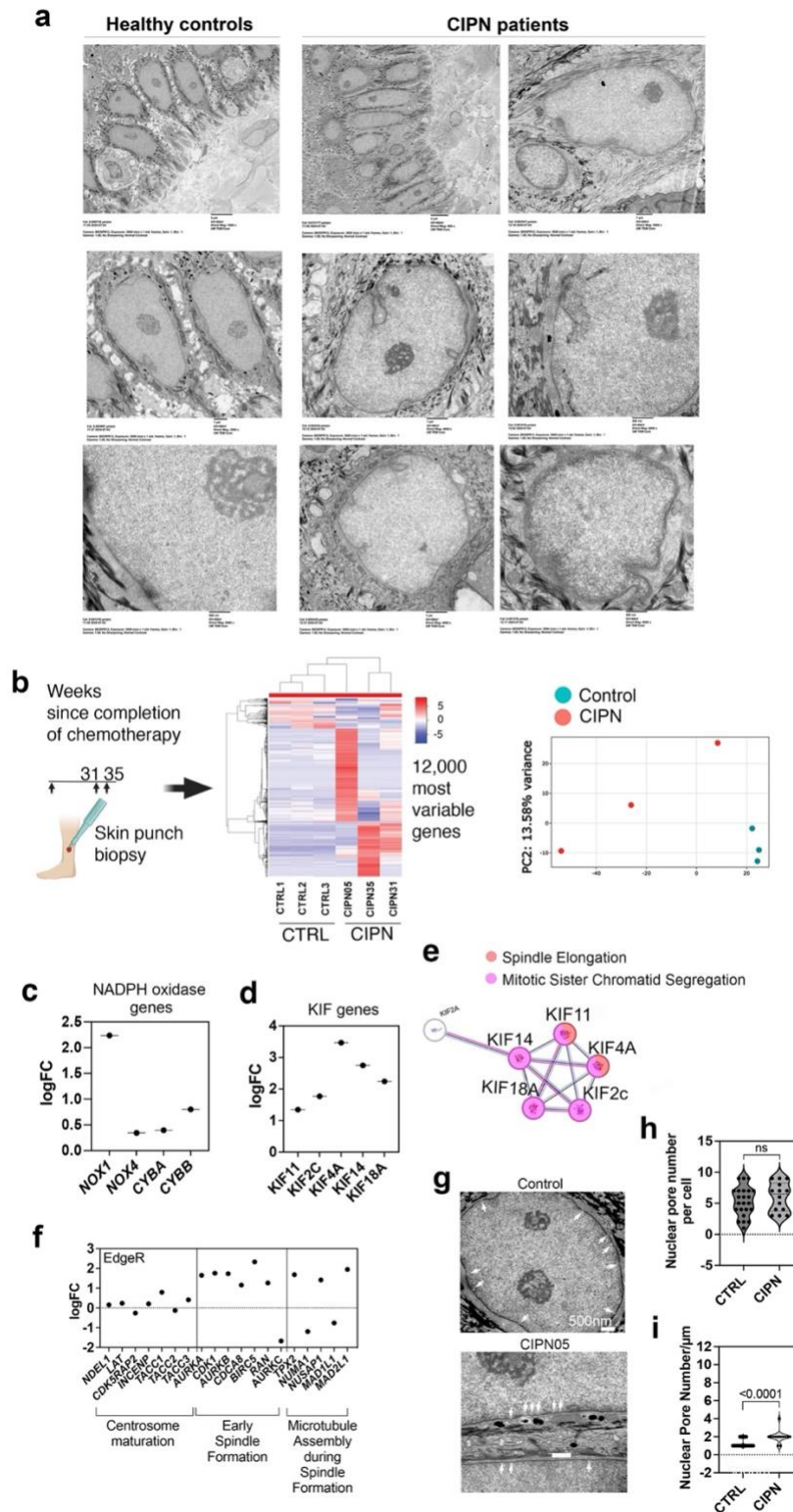


**Figure S11. Transmission electron microscopy and transcriptomic profiling of basal epidermal keratinocytes in CIPN patients and healthy controls.**

(a) Representative electron microscopy images of keratinocytes from control and CIPN patients. Nuclear invaginations and chromatin condensation are present in both groups but appear more pronounced in CIPN samples.

(b) RNAseq of lower leg skin from three CIPN patients (CIPN05, 31, 35) and three controls (CTRL1–3). Heatmap and PCA plot show distinct clustering of CIPN samples.

- (c) EdgeR analysis identifies co-upregulation of NADPH oxidase-related genes: *NOX1*, *NOX4*, *CYBA*, and *CYBB*.
- (d) Co-upregulation of mitotic kinesins: *KIF11*, *KIF2C*, *KIF4A*, *KIF14*, and *KIF18A*.
- (e) STRING network analysis shows *KIF11* interactions with other kinesins from (d).
- (f) Genes involved in different stages of mitosis are elevated in CIPN patient skin.
- (g) Electron microscopy reveals increased nuclear pore density in CIPN patient keratinocytes compared to controls.
- (h, i) Quantification of nuclear pore density confirms significant elevation in CIPN samples.

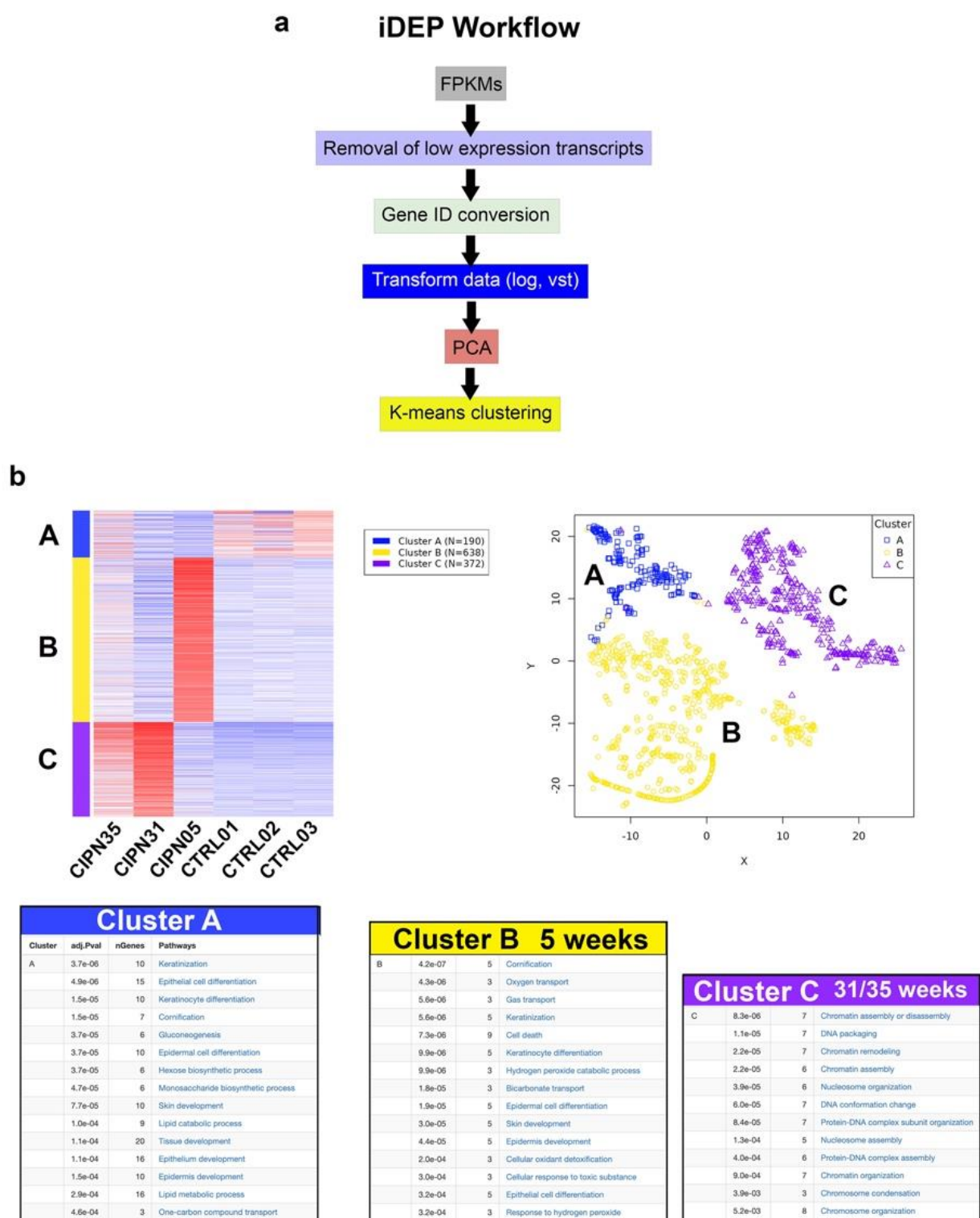


**Figure S12. Paclitaxel treatment upregulates cell cycle regulators in the skin of CIPN patients.**  
**(a)** Workflow for RNAseq analysis using iDEP, based on the previously published dataset (Staff et al., *Cancers* 2023).  
**(b)** iDEP clustering analysis of the top 1,200 most variably expressed genes reveals three distinct gene expression clusters. Cluster A (blue): Genes consistently downregulated in all three CIPN patients. Cluster B



(yellow): Genes uniquely upregulated in the patient diagnosed with CIPN at 5 weeks. Cluster C (purple): Genes upregulated in patients diagnosed with CIPN at 31 and 35 weeks.

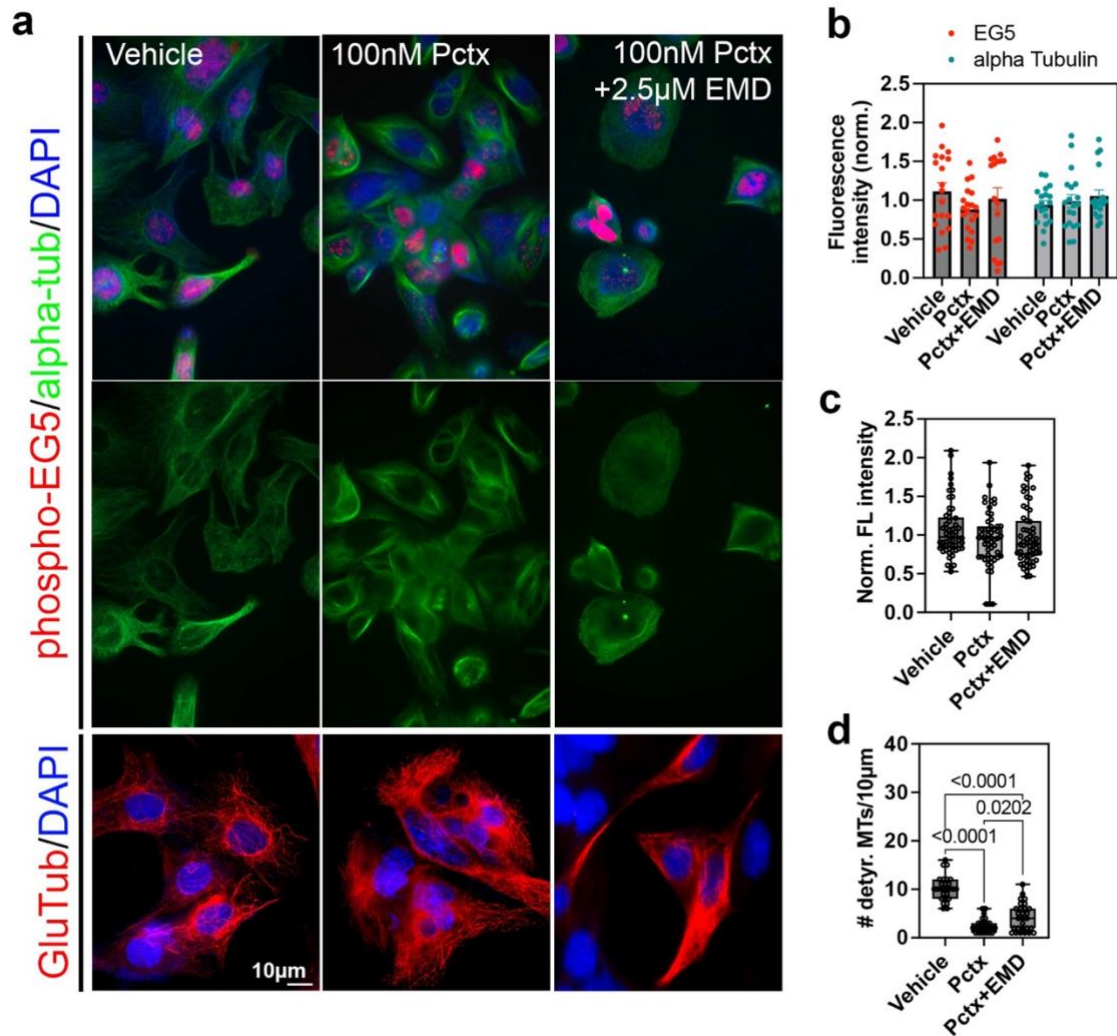


**Figure S13. EG5-dependent microtubule fasciculation in PC12 neurons.**

(a) Immunofluorescence images showing phospho-EG5, alpha-tubulin, and DAPI (top panel), and GluTub with DAPI (bottom panel).

(b) Quantification of phospho-EG5 fluorescence intensity shows no significant differences between vehicle, paclitaxel, and paclitaxel+EMD534085 groups.

(c) Normalized fluorescence intensity of deetyrosinated microtubules (GluTub) does not differ significantly among the treatment groups.

(d) Quantification of dMT fluorescence peaks along a 10µm line adjacent to the nucleus reveals fewer dMT bundles in paclitaxel-treated cells due to increased fasciculation. Co-administration of EMD534085 significantly rescues this phenotype.

## Supplemental Movie Legends

### **Movie S1. Mesenchymal cell morphology.**

3D rendering of detyrosinated microtubules (magenta) in a mesenchymal cell, with the nucleus shown in blue.

### **Movie S2. Detyrosinated microtubules in a vehicle-treated zebrafish caudal fin.**

96hr vehicle-treated zebrafish (6dpf) showing anti-GluTub-labeled detyrosinated microtubules and Hoechst 33342-labeled nuclei. Detyrosination is primarily observed in mesenchymal cells, which exhibit elongated microtubules spanning multiple keratinocytes. Mesenchymal nuclei are jagged and elongated compared to the rounded keratinocyte nuclei.

### **Movie S3. Detyrosinated microtubules in a paclitaxel-treated zebrafish caudal fin.**

Anti-GluTub and Hoechst 33342 staining of a 96hr paclitaxel-treated zebrafish (6dpf) reveal fasciculated dMTs looping around keratinocyte nuclei at the fin periphery.

### **Movie S4. Fasciculated dMTs interacting with keratinocyte nuclei.**

3D surface rendering of fasciculated detyrosinated microtubules (dMTs) and Hoechst 33342-labeled nuclei in the caudal fin following 96hr paclitaxel treatment. The dMTs contact the surface of a rendered keratinocyte nucleus.

### **Movie S5. Nuclear constriction by fasciculated dMTs.**

3D rendering shows fasciculated detyrosinated microtubules pinching off nuclear content in a keratinocyte nucleus after 96hr paclitaxel treatment.

### **Movie S6. Nuclear perforation by fasciculated dMTs.**

3D rendering of fasciculated dMTs and Hoechst-labeled nuclei demonstrates dMTs perforating the nuclear envelope following 96hr paclitaxel treatment.

### **Movie S7. dMTs traversing the nuclear lamina.**

3D rendering using Lamin B immunostaining (blue) and GluTub tracing (magenta) illustrates fasciculated dMTs crossing and perforating the nuclear lamina following 96hr paclitaxel treatment.

### **Movie S8. Live imaging of cell division.**

Time-lapse recording of mitotic events (blue arrows) in the caudal fin of a 6dpf Tg(h2a:h2a-GFP) transgenic zebrafish larva.

### **Movie S9. Nox1 localization in vehicle-treated zebrafish.**

3D rendering of Nox1 staining in an epidermal keratinocyte of a 7dpf zebrafish after 120hr vehicle treatment (0.05% DMSO starting at 2dpf). Nox1 localizes to the cytoplasm and nucleus.

### **Movie S10. Nox1 localization in paclitaxel-treated zebrafish.**

3D rendering of Nox1 staining in an epidermal keratinocyte of a 7dpf zebrafish following 120hr paclitaxel treatment (22  $\mu$ M starting at 2dpf). Nox1 localizes to the plasma membrane and forms clusters within the nucleus.

## Extended Materials and Methods

### Zebrafish embryo CRISPR microinjection protocol (IDT)

CRISPR-Cas9 knockouts were performed using the Alt-R™ CRISPR-Cas9 System (IDT) according to a protocol provided by Dr. Jeffrey Essner (Iowa State University). Alt-R crRNA and tracrRNA were each resuspended in Nuclease-Free IDTE Buffer to a final concentration of 100μM. To generate the gRNA duplex, 3μL of 100μM crRNA and 3μL of 100μM tracrRNA were mixed with 94μL of Duplex Buffer (IDT), followed by heating at 95°C for 5 minutes and cooling to room temperature (15–25°C). This yielded a 3μM gRNA stock, with final crRNA and tracrRNA concentrations of 36ng/μL and 67ng/μL, respectively. Cas9 protein (10μg/μL) was diluted to 0.5μg/μL in Cas9 working buffer (20 mM HEPES, 150 mM KCl, pH 7.5). For RNP complex formation, 3μL of the gRNA duplex was combined with 3μL of diluted Cas9 protein and incubated at 37°C for 10 minutes before cooling to room temperature. At the 1-cell stage, zebrafish embryos were injected with 3nL of the RNP mixture. At least 15 embryos were injected per condition, with 5 uninjected controls included. Toxicity was assessed at 8hr, and 1, 2, and 4 days post-fertilization. At day 4, genomic DNA was isolated using the NaOH lysis method. Pools of five embryos were lysed per tube, and three replicate pools were prepared for each condition, along with one uninjected control pool. The targeted region was PCR-amplified and run on 2% agarose gels to assess mutagenesis efficiency. Mutation frequencies were estimated by gel band pattern, sequencing, or T7 endonuclease I mismatch cleavage assays.

### Cell culture

The MDA-MB-231 human breast adenocarcinoma cell line was obtained from the American Type Culture Collection (Manassas, VA, USA) and cultured in Dulbecco's modified Eagle's medium (DMEM) (Corning) with 10% fetal bovine serum (FBS) and 1% penicillin/streptomycin (Cytiva). Wells were pre-coated with poly-L-lysine (Thermo Fisher) and plated cells incubated at 37°C, 5% CO<sub>2</sub>, and 95% humidity. At 50% confluency, the cells were treated with 200nM paclitaxel (Sigma-Aldrich), and some wells received 100nM EMD534085 (MedChemExpress, Cat. No. HY-15000) in addition to 200nM paclitaxel for 24 hours. The cells were subsequently fixed with 4% paraformaldehyde (PFA) for 15 min at room temperature for immunostaining. The PC12 cell line (derived from rat pheochromocytoma) was obtained from ATCC (USA). Cells were cultured in RPMI-1640 medium (Gibco) and supplemented with 10% fetal bovine serum (Gibco), 5% horse serum (Gibco), and 1% penicillin-streptomycin (Gibco). Cells were maintained in a humidified atmosphere at 37°C with 5% CO<sub>2</sub>. To induce differentiation into neurons, PC12 cells were seeded onto glass coverslips in 12-well plates at a density of 5x10<sup>4</sup> cells/well in three wells and biological replicates. Nerve Growth Factor (NGF, Sigma-Aldrich) was added to the medium at a concentration of 100 ng/mL, and cells were incubated for 5 days with medium changes every 2 days. Neuronal differentiation was confirmed by morphological changes, such as neurite outgrowth. Treatments were performed by adding paclitaxel (Paclitaxel, Sigma-Aldrich) at a final concentration of 100nM to the culture medium, in the presence or absence of EMD534085 (EMD, MedChemExpress, Cat. No. HY-15000) at concentrations ranging from 0.1 to 1μM for 24 hours. Matching DMSO concentrations were used as vehicle control.

### Immunofluorescence staining

Breast cancer cells: Following fixation, the cells were washed, permeabilized, and stained for rabbit detyrosinated microtubules (1:250 anti-GluTub, Sigma-Aldrich, Cat. No. AB3201), and mouse alpha-Tubulin (1:250 A Proteintech, Cat. No. 66031) overnight at 4°C, as described for zebrafish and mice. This was followed by secondary antibody staining using anti-rabbit Alexa Fluor 488 (Abcam, Cat. No. ab150077, 1:1000) and anti-mouse Alexa-Fluor 594 (Abcam Cat. No. ab150116, 1:1000) antibodies for 1 hour at room temperature, followed by 10 min DAPI staining. The wells were washed in 1xPBS 3x 5 minutes and imaged.

PC12 cells: Following treatment, cells were fixed with 4% paraformaldehyde (Thermo Scientific) overnight and then washed three times with phosphate-buffered saline (PBS, Corning). Specimens were permeabilized with 0.1% Triton X-100 (Sigma-Aldrich) in PBS for 5 minutes, followed by blocking in 5% bovine serum albumin (BSA, Sigma-Aldrich) in PBS for 1 hour. Primary antibodies were incubated overnight at 4°C. After three washes with PBS, samples were incubated with Alexa Fluor-conjugated secondary antibodies for 1 hour at room temperature in the dark. Samples were mounted onto glass slides using anti-fade mounting medium with DAPI (Thermo Fisher Scientific). The antibodies used were mouse anti alpha tubulin (Proteintech), rabbit anti



detyrosinated tubulin (Millipore), rabbit anti phospho-KIF11 (Thermo Fisher Scientific), Alexa 488 donkey anti-mouse (Thermo Fisher Scientific), and Alexa 555 donkey anti-rabbit (Thermo Fisher Scientific).

### Imaging

Stained breast cancer cells were imaged on a Zeiss LSM 880 Airyscan confocal microscope, Zeiss 20x Plan-Apochromat objective lens corrected for air, and 1x zoom. Sections (~3-5 per stack) were set to 1µm thickness and scan speed of ~800ms. The resolution was set to 1024x1024 pixels, and line scans with 4 lines averaged were recorded for each image.

PC12 cells were imaged using an inverted Zeiss Axio Observer Z1 equipped with a Plan-Apochromat 100×1.4na oil immersion objective lens. Fluorescent images were captured using a monochrome Zeiss AxioCam MRm CCD camera and processed with AxioVision 4.8 software. Post-acquisition adjustments, including brightness and contrast enhancements, were performed using NIH ImageJ software to optimize visualization and ensure accurate analysis of the fluorescent signals.

### Quantification

Fluorescence staining was analysed in FIJI. First, the images were background subtracted.

Breast cancer cells were assessed for presence of fasciculated dMTs using three wells and three biological replicates. The number of these cells/image was quantified and compared among treatment groups. One-way ANOVA was used for statistical analysis.

For PC12 cell fluorescence intensity measurements, the background was subtracted and fluorescence intensities (mean grey value) of all images from the three treatment groups were averaged. This mean fluorescence intensity value was subtracted from each data point to normalize for differences. For EG5/alpha-tubulin quantifications, the mean grey value was measured in the five brightest spots (EG5) or regions (tubulin) in each cell. For quantification of microtubule fasciculation, a 10µm line was drawn in parallel to the nucleus in representative cells stained for GluTub. The FIJI “Plot Profile” tool was used to quantify the number of the fluorescent peaks along the line. For each measurement, a background threshold was set that was present along the profile line. More peaks indicated more microtubules or thinner fasciculated bundles and less peaks indicated more fasciculation with thicker bundles.

### Python Code to generate polar plots

Polar plots were generated using Measurement points in Imaris to trace the X/Y coordinates (position) of microtubules. The positions were subsequently processed in Python to generate the polar plots using the following code:

```
import numpy as np
import matplotlib.pyplot as plt
import matplotlib as mpl
import sys, math
from locale import atof

def colorFader(c1,c2,mix=0): #fade (linear interpolate) from color c1 (at mix=0) to c2 (mix=1)
    c1=np.array(mpl.colors.to_rgb(c1))
    c2=np.array(mpl.colors.to_rgb(c2))
    return mpl.colors.to_hex((1-mix)*c1 + mix*c2)

# setting the axes projection as polar
ax = plt.axes(projection = 'polar')

S = 5
max = 0.0
with open(sys.argv[1]) as f:
    c = 0
    l = f.readline()
    while (l):
```

```

if l[0] == ' ':
    c += 1
    S[c] = []
    l = (f.readline()).split()
    x_0 = atof(l[0])
    y_0 = atof(l[1])
    S[c].append((0.0, 0.0))
else:
    S[c].append((atof(l[0]) - x_0, atof(l[1]) - y_0))
    l = (f.readline()).split()
c1='black'
c2='grey'

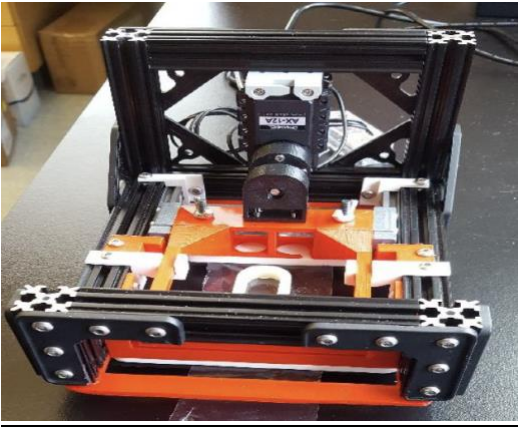
for x in S.keys():
    color = colorFader(c1,c2,x/c)
    X = list()
    Y = list()
    for rad in S[x]:
        x_1 = rad[0]
        y_1 = rad[1]
        if x_1 != 0:
            r = math.sqrt(x_1*x_1 + y_1*y_1)
            t = math.atan(y_1/x_1)
            if r > max:
                max = r

            X.append(t)
            Y.append(r)
            #plt.polar(t, r, color = 'black', linestyle='dashed', marker='k.', markersize=3)
        else:
            #plt.polar(0, 0, color = 'black', linestyle='dashed', marker='k.', markersize=3)
            X.append(0)
            Y.append(0)
    plt.polar(X, Y, 'k.', zorder=3, markersize=0, linestyle='solid', linewidth = 1.0, color = color)

#display the Polar plot
plt.show()

```

## ZStretcher User Manual



### Contents

Overview

Components & Materials

Device Set-Up

LabVIEW Operation

Notes

### **Overview**

With most of the components being 3D printed, the platform can be reprinted to match various stage inserts for confocal microscope, but the version below is shown for common Zeiss confocal microscope stages. The LabVIEW program that runs the motor must be installed on whichever device will be used with the controller (either the microscope's desktop computer or a laptop computer). There should be no need to access the block diagram of the LabVIEW program, as modifications to the block diagram will alter the calibrations of the motor operation.

### Components & Materials

Film & Mount

Film Blueridge Films, Inc. BFI-1880 Metallocene

Silicone grease and embedding agarose gel

3D PLA dividers: zfish chamber – \_horizontal/vertical/double partition.stl

Frame

Beams and Joints from OpenBeamUSA.com

Constructed by previous teams at UMaine

Bolts tightened with 5/64 hex/allen key

Sliding Platform

3D PLA prints attached to metal sliding brackets

Retained from the 3rd version of the model

Original manual caliper saved

Bolt Housing

3D PLA print: motor base.stl

(1) M5-.8 T-Nut and (4) M2-.4 screws

Fasteners

(2) 5mm tall 3D PLA prints

(2) 2mm tall 3D PLA print: fasteners.stl

(4) Original hex bolts and wing nuts

Stepper Motor

Electronics

Dynamixel AX-12A and Servo Manager Kit from Trossen Robotics

U2D2 Controller, 12V 5A power supply, AX/MX power hub 200mm 3 pin cables, power jack adapter, USB M-F cable

Hardware

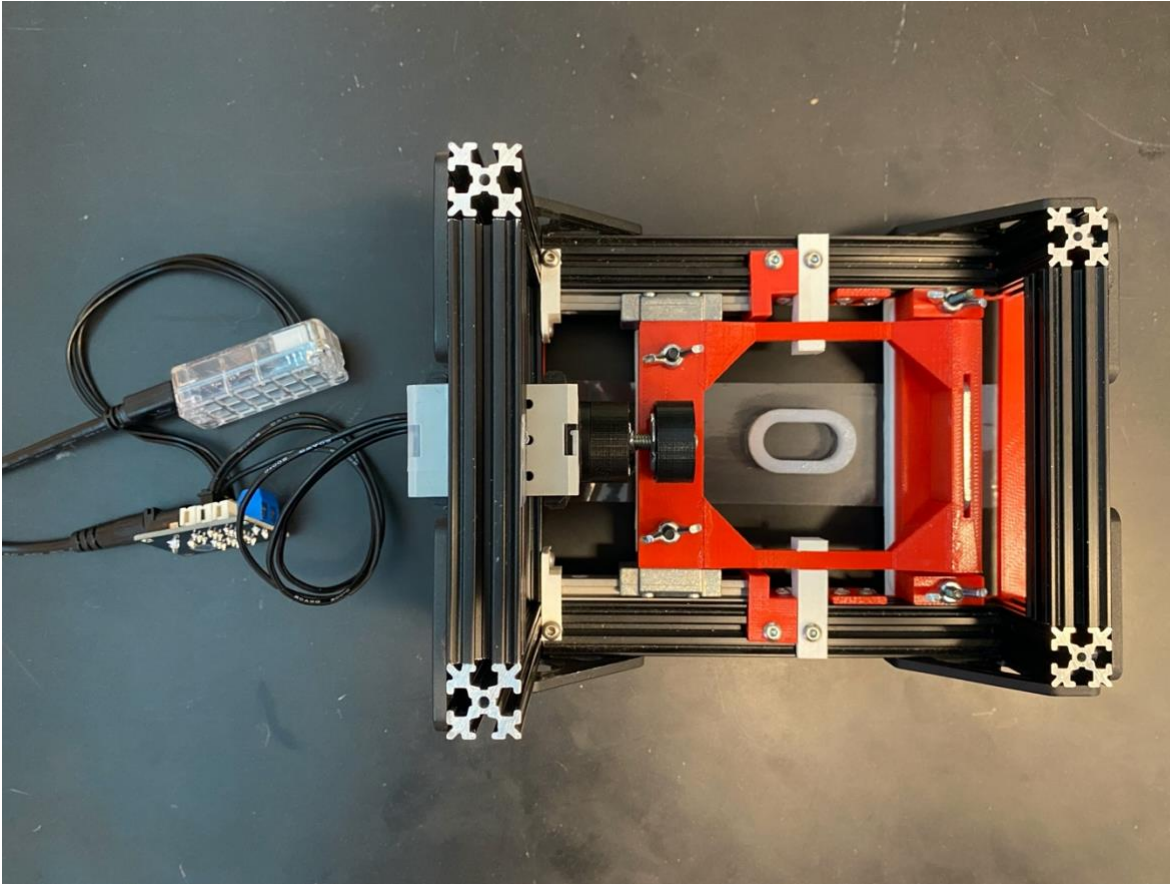
(1) 3D PLA adapter: motor attachment.stl

(1) M5-.8 25mm bolt, (1) M5-.8 T-Nut, (4) M2-.4 12mm bolts

(1) Dynamixel base, (2) OpenBeamUSA bolts, (4) M2-.4 5mm bolts

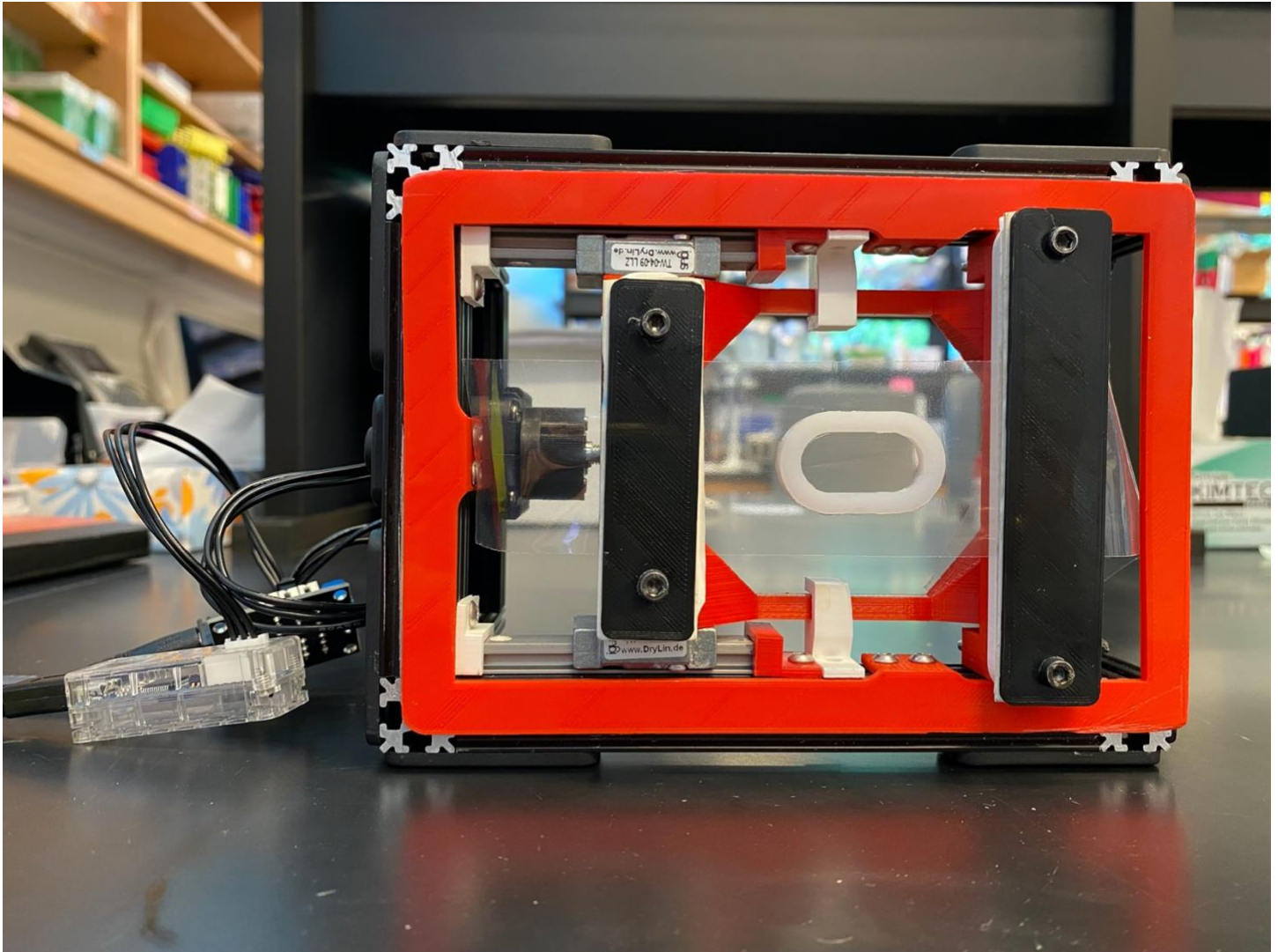
### Device Set-Up

The stretcher features a stationary clamp and a sliding clamp which is moved by a linear actuator to stretch a Metalocene film. The Dynamixel servo has a head attachment, which allows the bolt to be attached. Currently, a 25mm bolt is attached, but the attachment can be unscrewed and the 50mm bolt can be swapped into place if needed. The bolt has a 0.5mm diameter. The stepper motor, bolt, and bolt housing are all permanently attached to the device, so no set-up is needed.

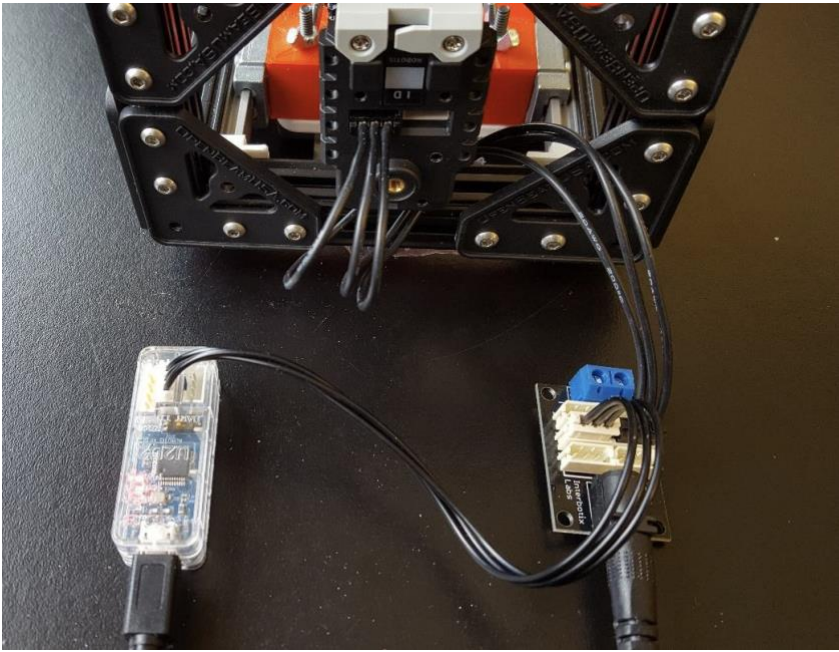




The film is fixed in place by plastic holders, and manually tightened by wing nuts and bolts. To insert the film between the white and black fasteners, the bolts from the bottom must be loosened. To stay within the working distance of the Zeiss Plan Neofluar 20X/0.50 Infinity objective, the black fasteners closest to the objective must be kept in place. However, do not tighten the fasteners entirely until the stepper motor is reset for maximal stretching.

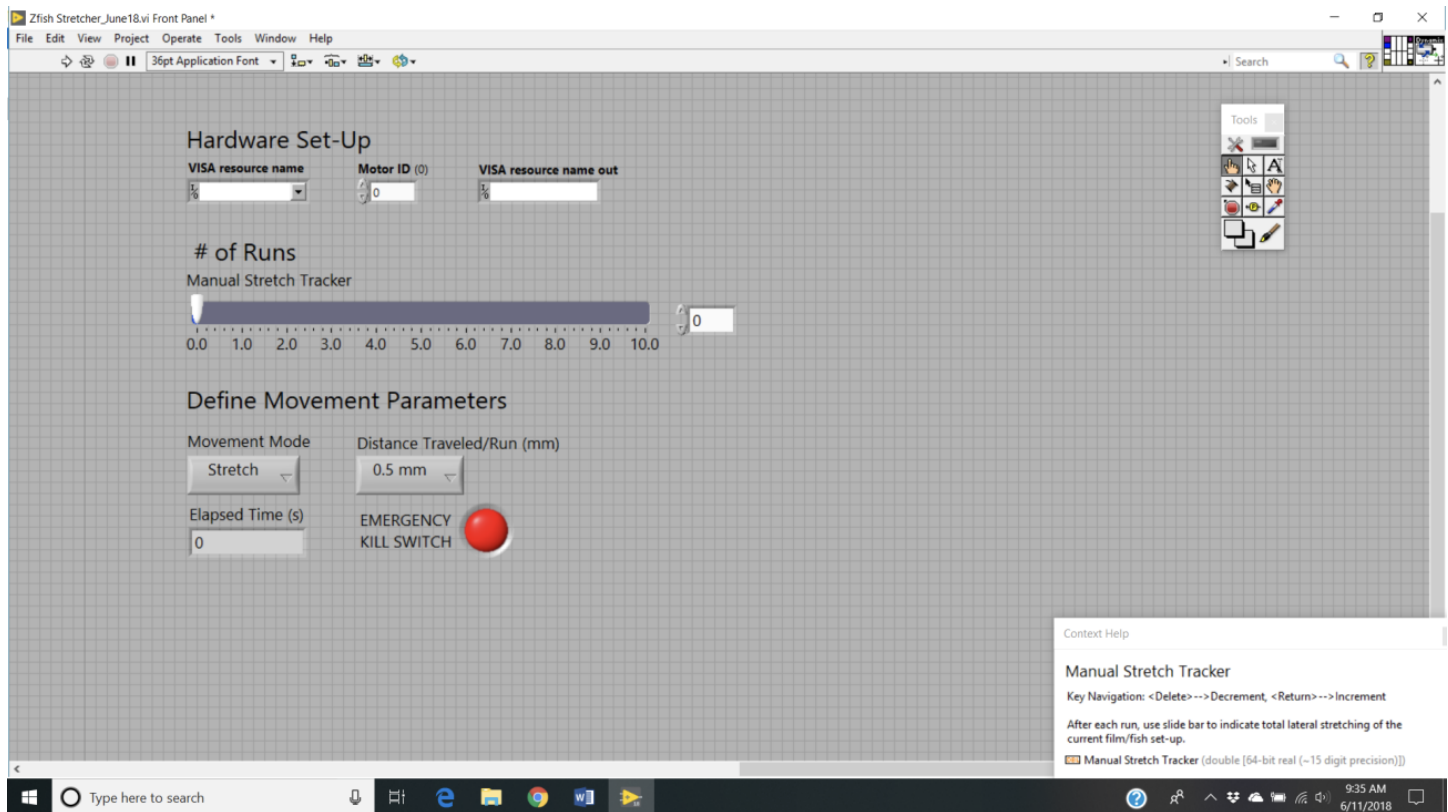


The stepper motor is controlled by a controller, a power hub, and a power supply. The black/black 3pin cable should be connected to the motor power hub as seen below. The U2D2 controller should be plugged into the power hub via the TTL port with the black 3pin cable seen below. The microUSB end of the USB cable should be inserted into the U2D2 controller, and the regular end of the USB cable should be inserted into the computer that is used for operation. The power supply should be plugged into a regular power outlet and into the power hub.

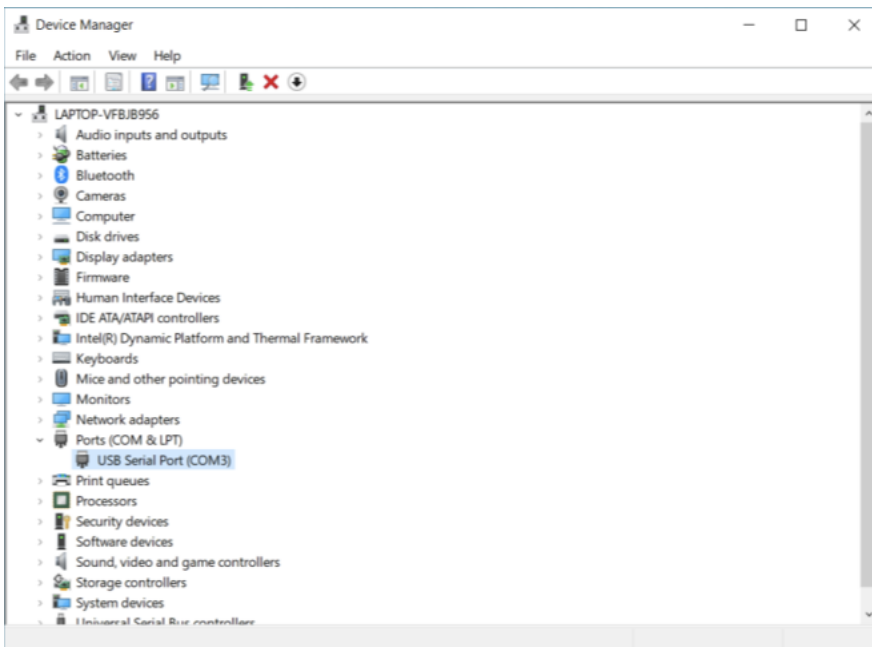


## LabVIEW Operation

The current virtual instrumentation file (.vi) is the ZStretcher\_June18.vi, which also requires the Dynamixel Setup sub.vi to operate. The Dynamixel library may not be included in the program upon startup, so the “dynamixel library” folder holds the .dll and .h files used by LabVIEW. It can be imported by selecting “Tools” → “Import” → “Shared Library” (use this link for directions: [LabVIEW](#)). Upon opening the ZStretcher\_June18.vi, the window below will appear. Annotated are the 9 essential tabs.



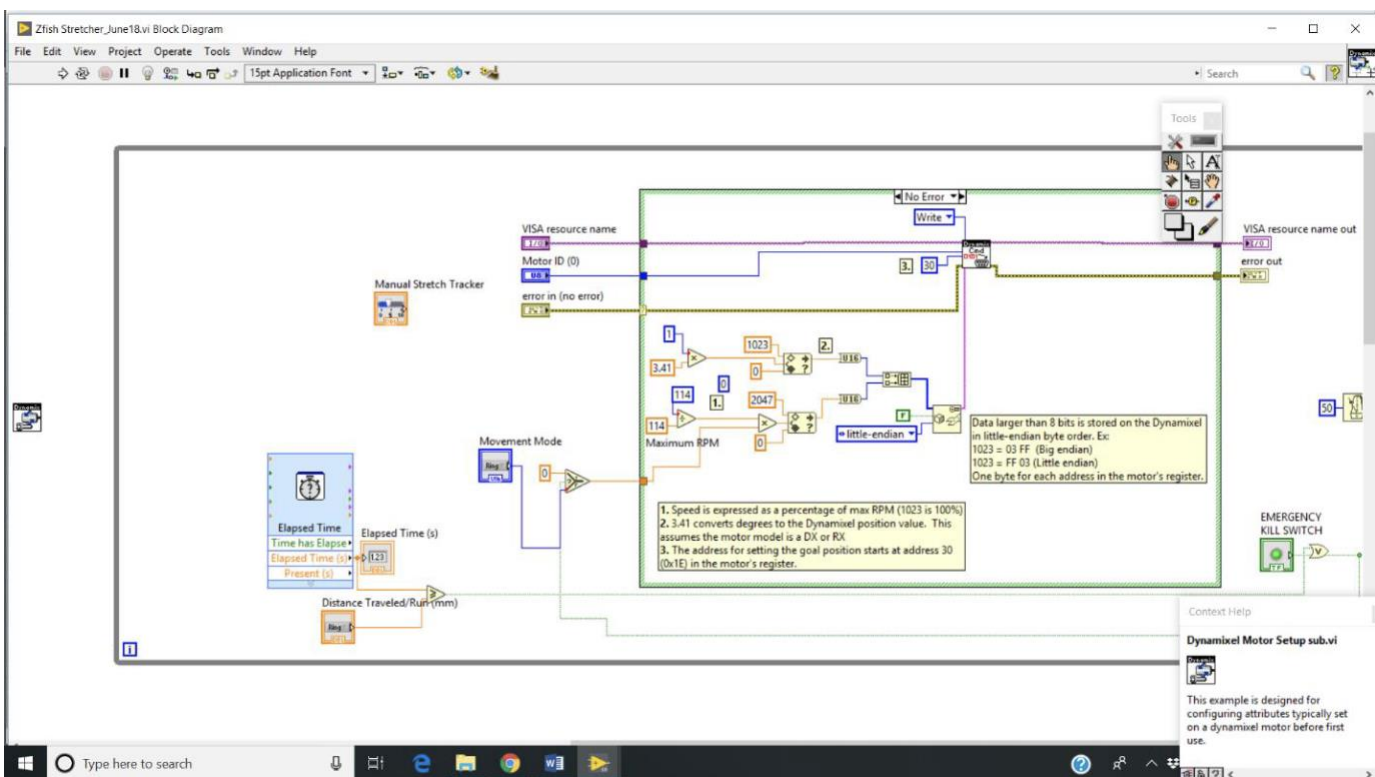
1. The arrow executes the program as defined on what is called the front panel
  - a. The front panel is simply the window shown.
  - b. Operations 6 & 7 define the operations that occur during a run/execution
2. The red circle is what ends each program, and must be selected at the end of each run
  - a. Clicking this button before the completion of the run/execution will result in a short circuit which causes the program to never stop
    - i. Should this happen, simply unplug the power sources and restart the program
3. The VISA resource name corresponds to the port on the computer which the controller, via the USB is plugged into
  1. This can be checked once the USB is plugged into your computer and accessing the device manager
  - b. Once in the device manager, click on “Ports” \_and see what port appears with the USB Serial Port



4. The Motor ID is what the .vi is currently calling the Dynamixel AX-12A.

a. The default is 0

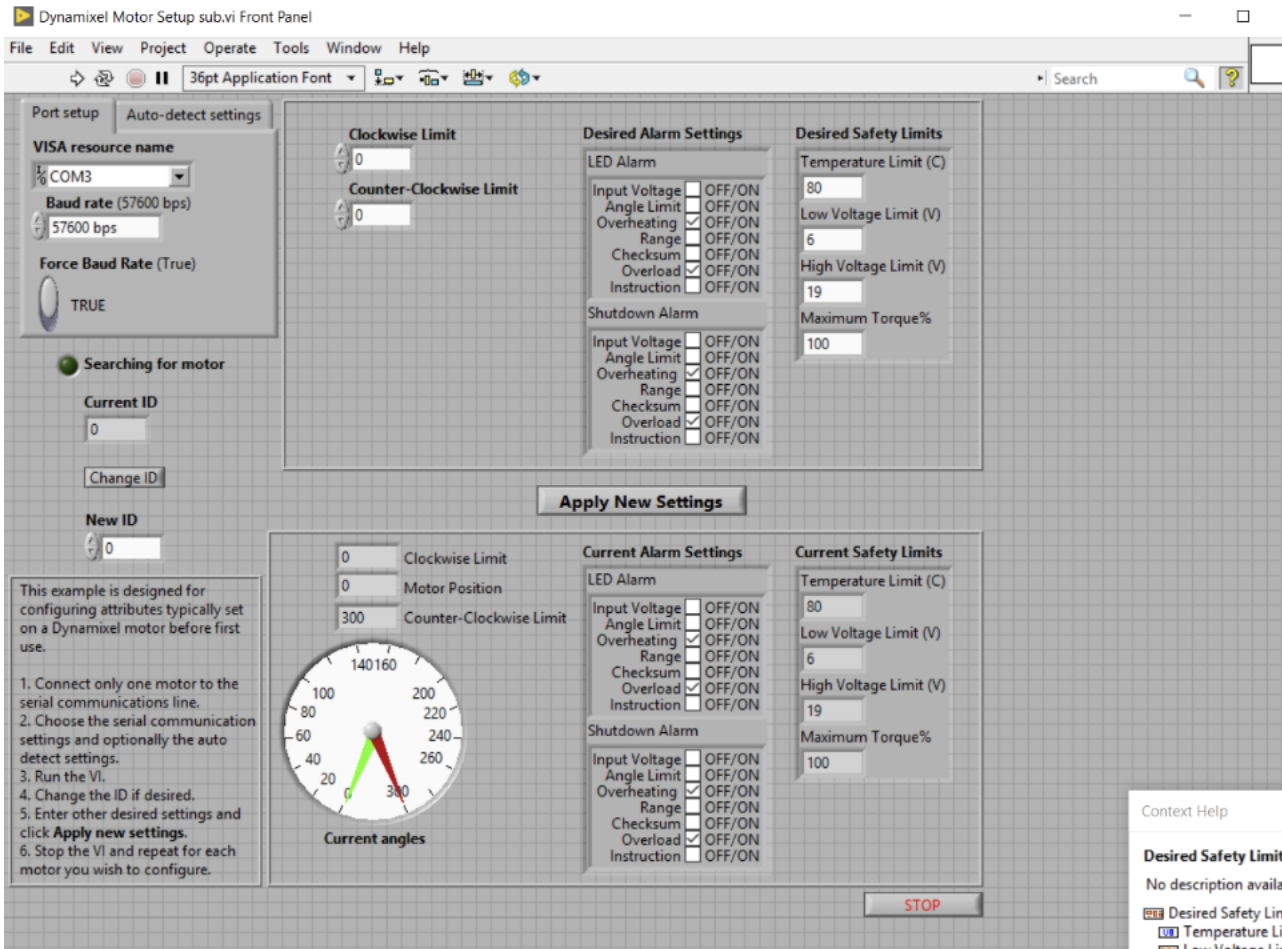
i. If the program never runs, open the control panel via clicking “Window” → “Show Block Diagram”



ii. Click on the box indicated, which is the sub.vi



iii. Check to make sure it is calling the motor 0, or manually correct

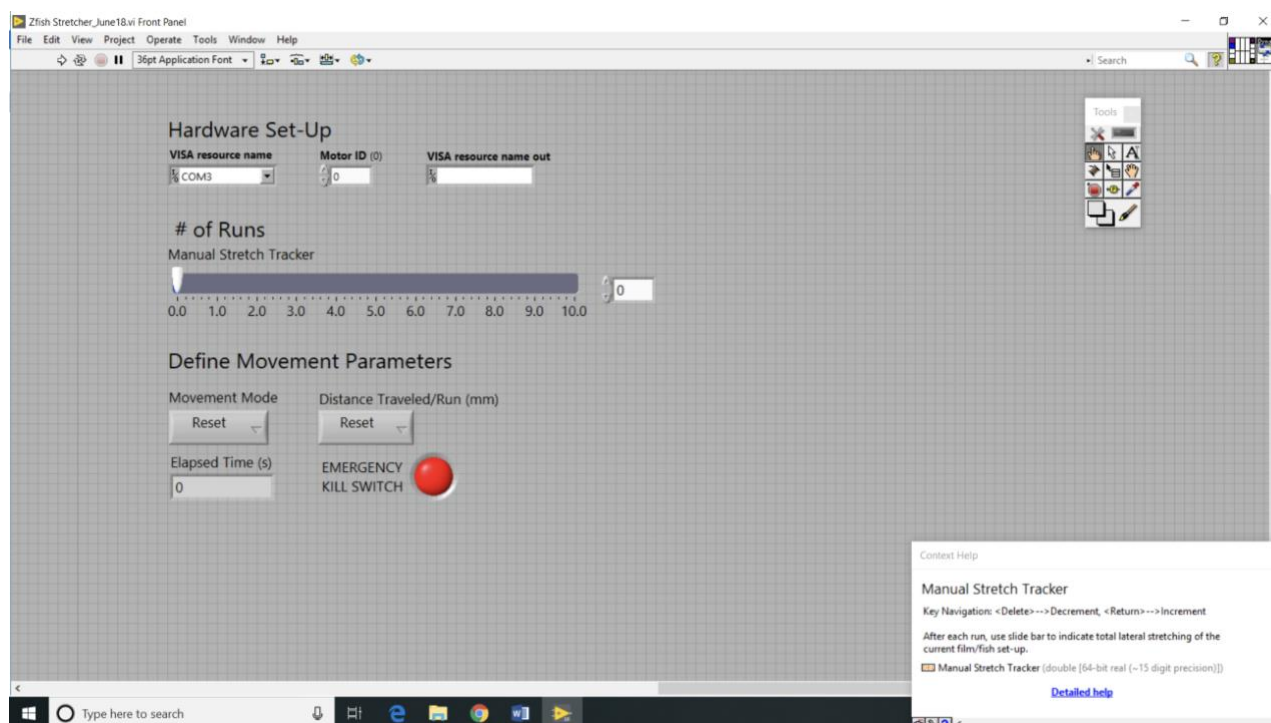


iv. After changing “New ID”\_to 0 and running the program, be sure to save

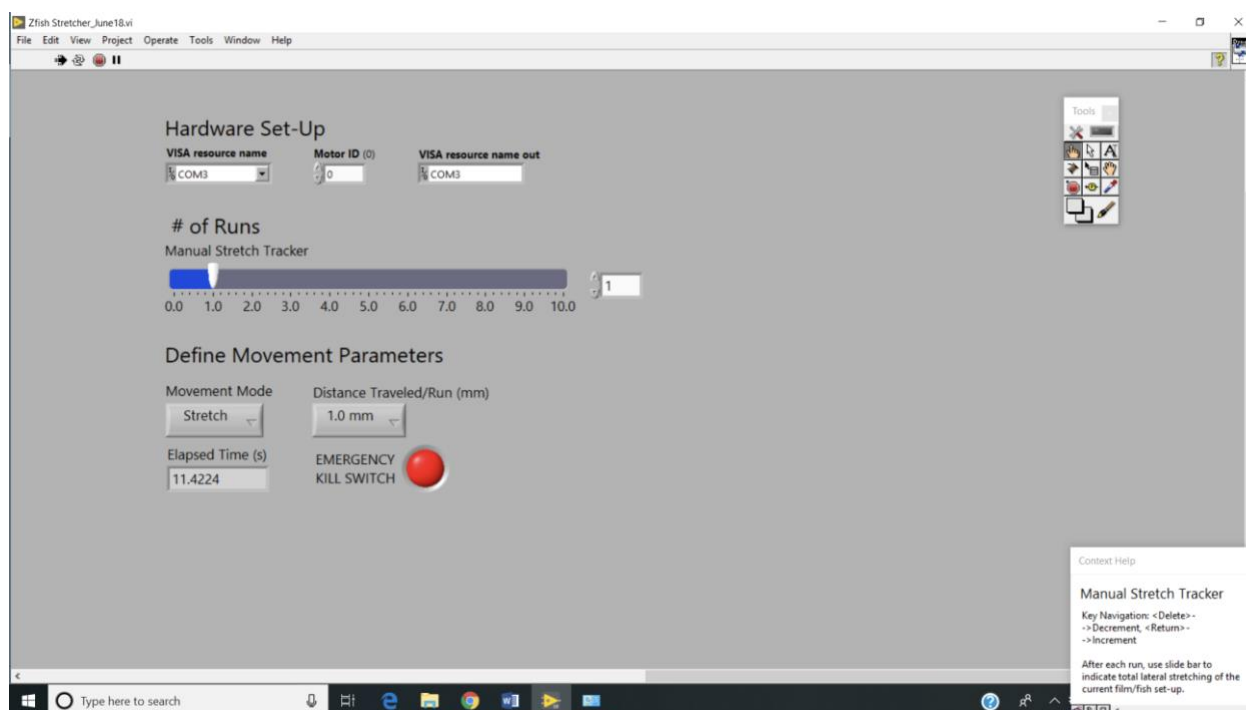
v. Exit the sub.vi and return to the main .vi

5. This is a manual indicator of how many runs/executions have been done on the current sample
  - a. Hit enter, or click on the up indicator, after each program run
  - b. At the end, you can simply multiply the # of runs by the number in box 7 to get the total distance travelled
6. Movement Mode is a click box to either stretch the fish or to reset the device to have the bolt moved back
  - a. Multiple runs may be needed to return the bolt to an optimal start position
7. The Distance Travelled/Run is a dropdown menu that includes 0.5/1.0/0.4/0.8/Reset options
  - a. Reset should be used with the Reset Movement Mode
  - b. It is advised that once you are in stretching mode, to only use one distance
8. Elapsed time indicates how long the program runs each time
  - a. Distance travelled is controlled by the RPM and time i. Each distance is set at the same RPM, but the time changes
    - ii. Ideal times are respectively 6.25/11.4/5.3/9.4/15 seconds
9. The Emergency Kill Switch can be clicked during the program to cease the run

You can scroll over the controls on the front panel and a description of each will appear in the bottom right text box on the screen. Before each experiment, it is wise to reset the bolt back so that it is barely in the housing/nut. This may need to be executed multiple times.

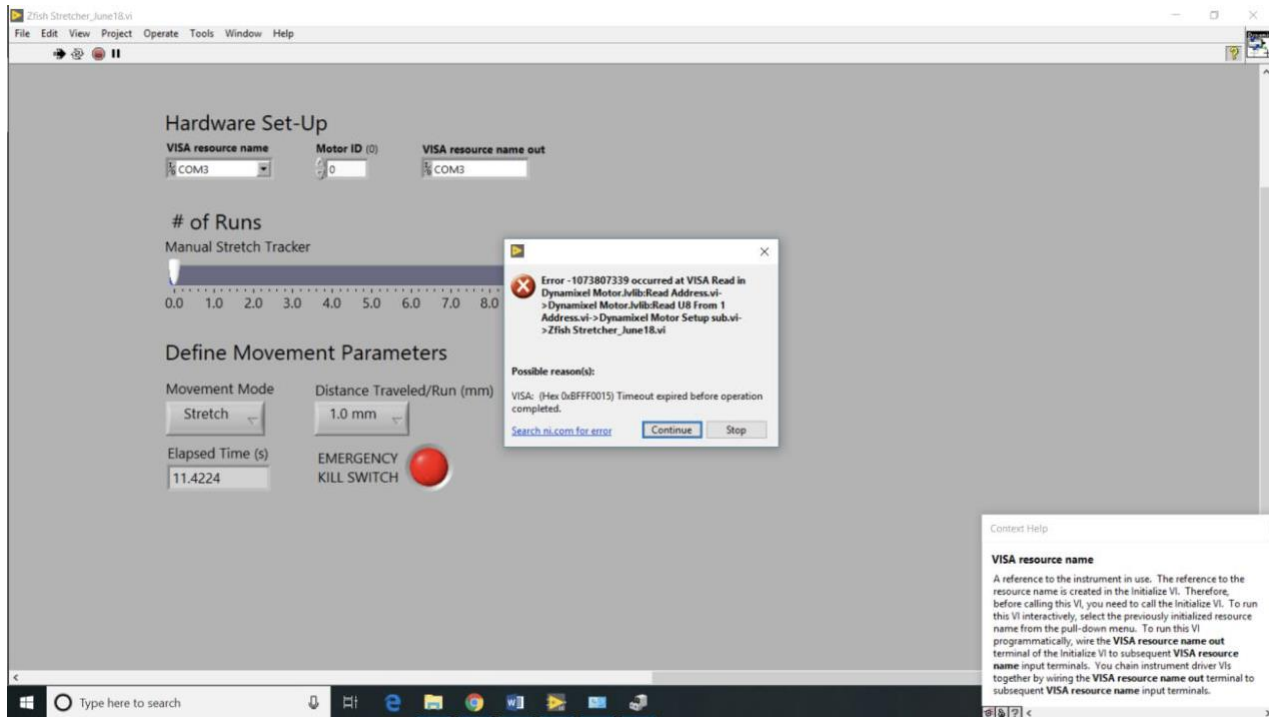


After the bolt is reset, you can then run the program on stretch mode and define your distance used per iteration. Be sure to mark the # of runs at the end of each execution.



This LabVIEW program has a bug that cannot be fixed, and which may depend on the version. A warning pop-up may appear (shown below) during the middle of your run that states that the control blocks cannot find the angle of the motor during the run. Since we use time to control distance, this error is irrelevant. Simply click on

“Continue” and the run will remain normal. However, if you click “Stop” or in rare instances, the motor will continue to spin, try the kill switch or unplug the power sources and restart the program.



## Notes

1. LabVIEW must be installed on whatever device is being used to operate the device.
2. Viewing the block diagrams is great to understand the of the program but be careful to not save unwanted edits.
3. View the [user manual](#) for the Dynamixel AX-12A.
4. Websites for [Trossen Robotics](#) and Metalocene BFI 1880 ([Blueridge Film](#)).
5. All hardware was purchased from Home Depot, printed with an UltiMaker 2
6. To periodically check the accuracy of the travel distance, run the 0.4mm or 0.8mm multiple times
  - The 0.4mm option should result in a  $\frac{1}{2}$  rotation of the motor and the 0.8mm should result in one full rotation of the motor
  - If adjustments are needed, right click on the Distance Travelled box and selecting “Date Entry”, then “Edit Items” will allow you to adjust the time corresponding to each distance.